Humidity Effect on the Drift Times of the Reactant Ions in Ion Mobility Spectrometry

Mahmoud Tabrizchi*[1], Helko Borsdorf[2], Zahra Izadi[1], Hossein Farrokhpour[1]

[1] *Department of Chemistry, Isfahan University of Technology, Isfahan, 84156-83111, Iran*

[2] *UFZ-Helmholtz Centre for Environmental Research, Department Monitoring and Exploration Technologies, Permoserstraße 15, 04318 Leipzig, Germany*

* Corresponding Author: Mahmoud Tabrizchi, m-tabriz@cc.iut.ac.ir

Abstract

The effect of moisture content on the drift times of NH_4^+ and H_3O^+ reactant ions at different temperatures was experimentally and theoretically studied using an ion mobility spectrometer (IMS). The peak positions of the ions shifted to higher drift times as the humidity of the drift gas increased. The peak displacements were attributed to the consecutive formation of hydrated ion clusters, $RI^+(H_2O)_n$. Using chemical equilibrium relations and thermodynamic data derived from DFT calculation, a model was proposed to formulate the change in the drift times as $1/t_d = 1/t_d^{\Theta} - \beta T \log[H_2O]$, where β is a constant and T is temperature. $[H_2O]$ is the concentration of water in ppm and, t_d^{Θ} is the drift time at the standard condition of $[H_2O]$=1 ppm. The proposed equation perfectly predicted the change in the drift times of the reactant ions as a function of the moisture in the drift gas. Accordingly, standard mobility, $K = K^{\Theta} - \gamma T \ln[H_2O]$, was defined, which is independent of the moisture level of the drift gas and reflects the chemical reactivity. In this work, it is proposed to correct the reported reduced mobilities for the moisture to a standard condition of 1 ppm water concentration, in a similar manner to the corrections to the standard temperature and pressure of 273 K and 760 mbar, respectively. Finally, the likelihood that different hydrates forms of the reactant ion exist is discussed based on the entropy concept.

Keywords: Ion mobility spectrometry; drift time; humidity; reactant ions, chemical potential

1. Introduction

Ion mobility spectrometry (IMS) is a fast, simple and sensitive technique with a wide range of applications in chemistry, pharmacology, clinical diagnosis, security and biomedical sciences[1,2]. IMS is a well-established technique for the detection of explosives[3,4], industrial chemicals[5], environmental pollution[6], chemical warfare agents[7,8] and many other volatile organic compounds [9]. The IMS detection technique is based on the measurement of the drift time or the mobility of ions produced from an analyte. The maxima of these peak occur at specific drift times depending on the mobility coefficient of the ions and the conditions of the experiment. IMS is extensively used in portable instruments, mainly for security purposes, that identify the target ions, based on drift time analysis and pattern recognition software. Any uncontrolled change in the drift time in those IMS-based detectors arising from changes to the experimental conditions, results in false alarms or missing threats.

It is well known that drift times are affected by the ambient temperature, pressure and humidity. The effects of temperature [10,11,12] and pressure [13,14] on the spectrum resolution, drift time behavior, and measurements in IMS have been well investigated by many researchers. The drift times are related to mobility values *K*, defined as;

$$K = \frac{v_d}{E} \qquad \text{(eq.1)}$$

where v_d is the drift velocity of the ion moving under the influence of the electric field, *E*, in the drift region. The drift velocity can be substituted to give $K=D/E.t_d$, where *D* is the drift length and t_d is the drift time. The *K* values are then simply corrected for the ambient temperature (*T*) and pressure (*P*) through Eq. 2

$$K_o = K \times \frac{273}{T} \times \frac{P}{760} \qquad \text{(eq. 2)}$$

The corrected mobility is called reduced mobility (K_o), which is ideally independent of the temperature and pressure [1]. However, there is no correction term for humidity in the reduced mobility equation, although the mobility is profoundly affected by the water content of the drift gas. The difference in the water content could be a significant source of discrepancy in the reported values for the reduced mobilities.

Moisture affects both, the drift times, and the appearance of ion mobility spectra. The effect of humidity on the performance of IMS with different ionization sources in the positive and negative modes has been studied by several research groups [15, 16, 17, 18, 19, 20]. These studies show that humidity affects both, the appearance of the ion mobility spectra and the peak positions, depending on the path where the moisture enters the IMS cell. Makinen et al. [15] investigated the effect of humidity on the ion mobility spectra of amines and their monomers and proton-bound dimers. They found that the protonated monomers are hydrated in the presence of water vapor while the dimers are not hydrated but destroyed. Vautz et al. studied the effect of moisture on the intensity of the peaks in an IMS equipped with a photoionization source [17, 18]. They found that the humidity reduces the efficiency of the ionization source so that the intensity of the positive product ions decreased with increasing

the humidity [17, 18]. Borsdorf et al. [19, 20] systematically investigated the influence of humidity in the carrier and drift gases on both the peak position within the ion mobility spectrum and quantification. They focused on the negative reactant ion $O_2^-(H_2O)_n$ and some halogenated substances as target compounds. It was reported that the moisture in the carrier gas affects only the ionization mechanism and the peak intensities, while increased humidity in the drift gas considerably shifts the peak positions. The changes in peak position were found to be nonlinearly dependent on the humidity and vary for the reactant ion and the halogenated substances. As a result, the peak-to-peak resolution and differences in drift times changed after introducing moisture. The shifts were attributed to the tendency to form ion-water clusters and to changes in the collisional cross-section and the composition of the gas. Recently, Zhang et al. studied the dependence of average mobility of ions in the air with pressure and humidity [21]. They also reported that the average mobility of air ions decreases with increasing humidity. A correction formula for the average mobility of ions in the air, taking account of humidity, was presented. However, it is not applicable to IMS since their moisture level was very high (relative humidity of 25%-75%) and no specific ion was studied. In addition, lately, Safaei et al. characterized the performance of a differential mobility spectrometer at ten values of water vapor concentration, from 100 to 17000 ppm for seven ketones [22]. They reported increased alpha functions (field-dependence of ion mobilities) for the reactant and product ions with increased moisture levels and decreased quantitative response.

As reported by other researchers, the humidity certainly changes the shape and positions of the peaks and influences the thermodynamics [23], kinetics [24] and the mechanism of the ion-molecule reactions occurring in IMS. Hence, it interferes with the detection of target substances in commercial IMS based detectors. Although the effect of humidity has been studied by several groups, a correction for deviations in drift times caused by the humidity content of the IMS cell has not yet been proposed. Given the problems that humidity can cause problem in the detection, a reliable correction formula for humidity is of great interest.

This work aims to deeply investigate the effect of humidity of the drift gas on the positions of the positive reactant ions in IMS. Furthermore, it is intended to formulate the peak shifts based on the thermodynamics of ion-molecule reactions and cluster formation. This formula can be used to correct the peak positions based on the humidity level.

2. Computational details

The structures of the neutral reactant ions, as well as the hydrated clusters, were fully optimized using density functional theory (DFT) employing CAM-B3LYP functional. The 6-311++G (d, p) basis set, which includes enough polarization and diffused function for hydrogen and heavy atoms was used for all calculations. Figure 1 shows the optimized structures of hydrated reactant ions, $NH_4^+(H_2O)_n$ and $H_3O^+(H_2O)_n$ in the gas phase up to 3 water molecules.

n	0	1	2	3

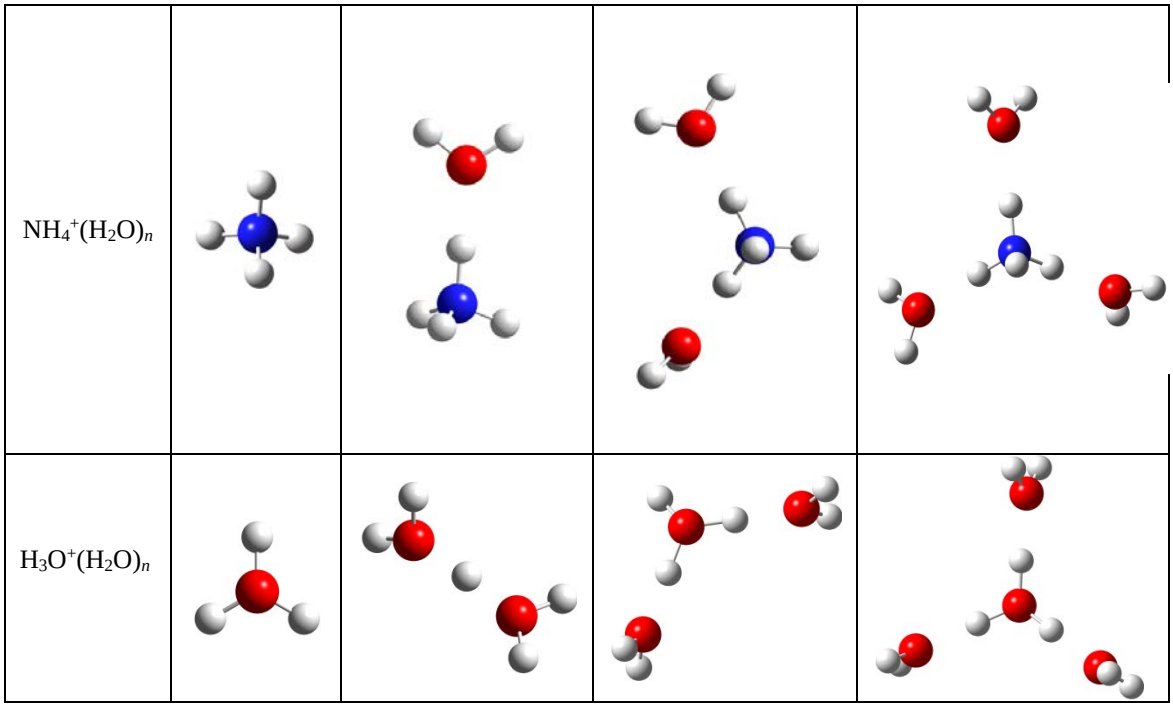

Fig. 1. The optimized structures of hydrated ammonium, $NH_4^+(H_2O)_n$, and hydronium $H_3O^+(H_2O)_n$ optimized by the CAM-B3LYP/6-311++G (d,p) computational method in gas phase.

The frequency calculations were performed at the same level of theory to obtain the thermodynamic quantities including $\Delta G°$ and $\Delta H°$ values at 298 K. The Gaussian 09 software [25] was employed for all calculations. The calculated values of ΔG^o and ΔH^o of the consecutive hydration of NH_4^+ and H_3O^+ (up to 5 water molecules) in the reaction of $X^+(H_2O)_n + H_2O \rightleftharpoons X^+(H_2O)_{n+1}$ for $X^+=NH_4^+$ and H_3O^+ have been tabulated in Table 1. This information is used to calculate the equilibrium constant of the reactions, as explained in the following sections.

Table1. The calculated ΔG^o and ΔH^o values of the consecutive hydration of X^+ (up to 5 water molecules) in reaction $X^+(H_2O)_n + H_2O \rightleftharpoons X^+(H_2O)_{n+1}$ where $X^+= NH_4^+$ and H_3O^+.

X	**NH_4^+**				**H_3O^+**			
	ΔG˚ (kcal/mol)		*ΔH˚(kcal/mol)*		*ΔG˚ (kcal/mol)*		*ΔH˚(kcal/mol)*	
n	this work	*NIST*	this work	*NIST*	this work	*NIST*	this work	*NIST*
0	-14.81	-	-22.40	-20.52	-30.43	-	-38.36	-32.38
1	-9.88	-8.81	-17.46	-17.33	-16.45	-	-23.43	-20.00
2	-8.34	-6.43	-13.96	-13.64	-9.67	-9.29	-19.30	-17.38
3	-6.09	-5.00	-12.22	-12.14	-6.28	-5.48	-13.96	-13.33
4	-2.68	-	-10.88	-10.57	-2.67	-4.5	-11.92	-11.90

3. Experimental

3.1. Ion mobility spectrometer

The ion mobility spectrometer used in this work was a desktop research-grade instrument manufactured in our lab at the Isfahan University of Technology. The IMS cell (16 cm in length) was constructed from aluminum rings including the ionization and the drift regions. The two regions were separated by a Bradbury-Nielson shutter grid with the opening time of 100 μs in 20 ms intervals. The IMS instrument is equipped with corona discharge (CD) [26] for generating of H_3O^+ and NH_4^+ ions. The drift field (*E*) was 437.5 V/cm, which was established by applying a potential of 7000 V throughout the cell. All experiments were carried out in the positive polarity. More details can be found in Ref. 27.

Purified nitrogen was used as the drift gas. The flow rate of the drift gas was typically 700 mL/min. There was no need for carrier gas, as no sample was used. Instead, a water vapor saturated gas was mixed with the drift gas to adjust the moisture level inside the drift tube. The experiments were carried out at ambient pressure and in a temperature range of 90-200 ^oC.

3.2. Adding moisture and its measurement

In order to increase the humidity of the drift region, a mixture of flows of dry gas and 100%, relative humidity was used. The humid gas was generated by bubbling a gas stream through a small vessel containing liquid water. This stream was then added to the flow of the drift gas. The amount of moisture entering into the drift gas was adjusted by varying the flow rate of the saturated gas. The final concentration of water in the drift cell was measured using a dew point meter (LPDT, Xentaur, USA) at the exit of the IMS cell. The moisture was measured at the exit gas to take into account for the ambient water vapor, diffused inside the IMS cell.

4. Results and discussion

4.1. Drift time shifts

Figure 2 shows the displacement of the ion mobility peaks of NH_4^+ and H_3O^+ reactant ions produced by the corona ion source in the presence of different moisture levels in the drift tube. The NO^+ peak is absent since nitrogen is used as the drift gas. Also, the commonly observed NO^+ peak in the presence of air disappears when water vapor is added. Hence, we just focused on the main two reactant ions, NH_4^+, and H_3O^+.

It is clear from Fig. 2 that, as the concentration of water increases, the peaks shift to the higher drift times. The shift is not equal for all peaks, so that at high water concentration, the two NH_4^+ and H_3O^+ peaks get closer together. For both peaks, the change in the drift time is faster at the low level of moistures, and it reaches a plateau at higher moisture levels. Such behavior is similar to that reported by Borsdorf et al. [19]

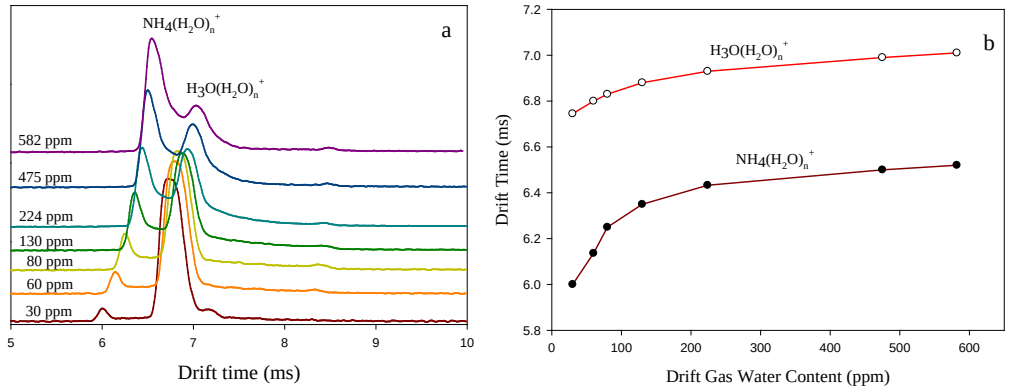

Fig. 2. The effect of water concentration on the displacement of the NH_4^+ and H_3O^+ reactant ions at 140°C. a) the reactant ion spectra, b) the drift times versus moisture level of the drift gas.

The peak shifts may be explained based on the change in the relative abundances of the reactant ion, $RI^+ (H_2O)_n$ clusters. At higher concentrations of water, the formation of hydrated ions with larger *n's* favors. At high moisture level, all ions are heavily hydrated; hence, no more hydration happens if the water content is further increased. Therefore, the peak shifting is stopped at a very high level of moisture. Another point is that the extent of hydration depends on the nature of the ion so that different ions shift differently. Hence, the peak-peak distance is also changed by adding moisture. Borsdorf et al also observed the change in the peak-peak resolution by humidity [19]. To formulate the relationship between peak resolution and humidity, the hydration of ions in the presence of water vapor must be taken into account in full detail. Here, the thermodynamics of common reactions for the reactant ions that take place in the drift tube will be considered.

4.2. Hydration of ions

Because of the presence of trace amount of water vapor in the IMS cell, the ion (M^+) is usually hydrated to $M^+ (H_2O)_n$, where, *n* is the number of water molecule participating in the hydration. In reality, a chain of hydration reactions occurs in the IMS cell. As a result, the number *n* is not constant and a variety of $M^+ (H_2O)_n$ with different *n*'s are produced. Since the ion-molecule reactions are very fast, the adjacent hydrated species (*n* and *n+1*) quickly reach a state of equilibrium. Hence, the hydration of M^+ in the IMS cell can be considered as a consecutive series of reactions; $M^+ (H_2O)_n + (H_2O) \leftrightarrow M^+ (H_2O)_{n+1}$. The equilibrium constant for the formation of $M^+(H_2O)_{n+1}$ is $K_n=[M^+(H_2O)_{n+1}]/[M^+(H_2O)].P_w$, where P_w is the partial pressure of water vapor. The relative abundances of the hydrated ions with different water molecules, *n*, depend on the nature of the core ion, as well as the temperature and the water content of the drift gas. In our earlier works [23, 24], an equation was introduced to give the mole fraction, X_n, of each hydrated ion in the mixture as;

$$X_{n+1} = P_w^{n+1} \prod_0^n X_0 K_n \qquad \text{(eq.3)}$$

Where, X_0 is the relative abundance of the non-hydrated ion, given as:

$$X_0 = \frac{1}{1+\sum_{n=0}^{\infty}(P_w^{n+1}\prod_{i=0}^{n}K_i)} \qquad \text{(eq.4)}$$

The equilibrium constants, K_i's, for a specific core ion, were obtained via DFT calculations of ΔG^o and ΔH^o using $K_i = \exp(-\Delta G_i^o / RT)$ at 298 K. The equilibrium constants at temperatures other than 298 K were obtained from the Clausius-Clapeyron relation [28]. The calculated logarithm of equilibrium constants for the H_3O^+ and NH_4^+ are presented in Table S1-2. Having the equilibrium constants, one may calculate the mole fractions for each reactant ion. The mole fraction of the $H_3O^+(H_2O)_n$ and $NH_4^+(H_2O)_n$ clusters as a function of temperature at different water vapor levels are shown in the supporting material (Fig.S1-2). The mole fractions for different components of $NH_4^+(H_2O)_n$ and $H_3O^+(H_2O)_n$ ions at different water vapor levels for two temperatures, as an example, are presented in Fig. 3.

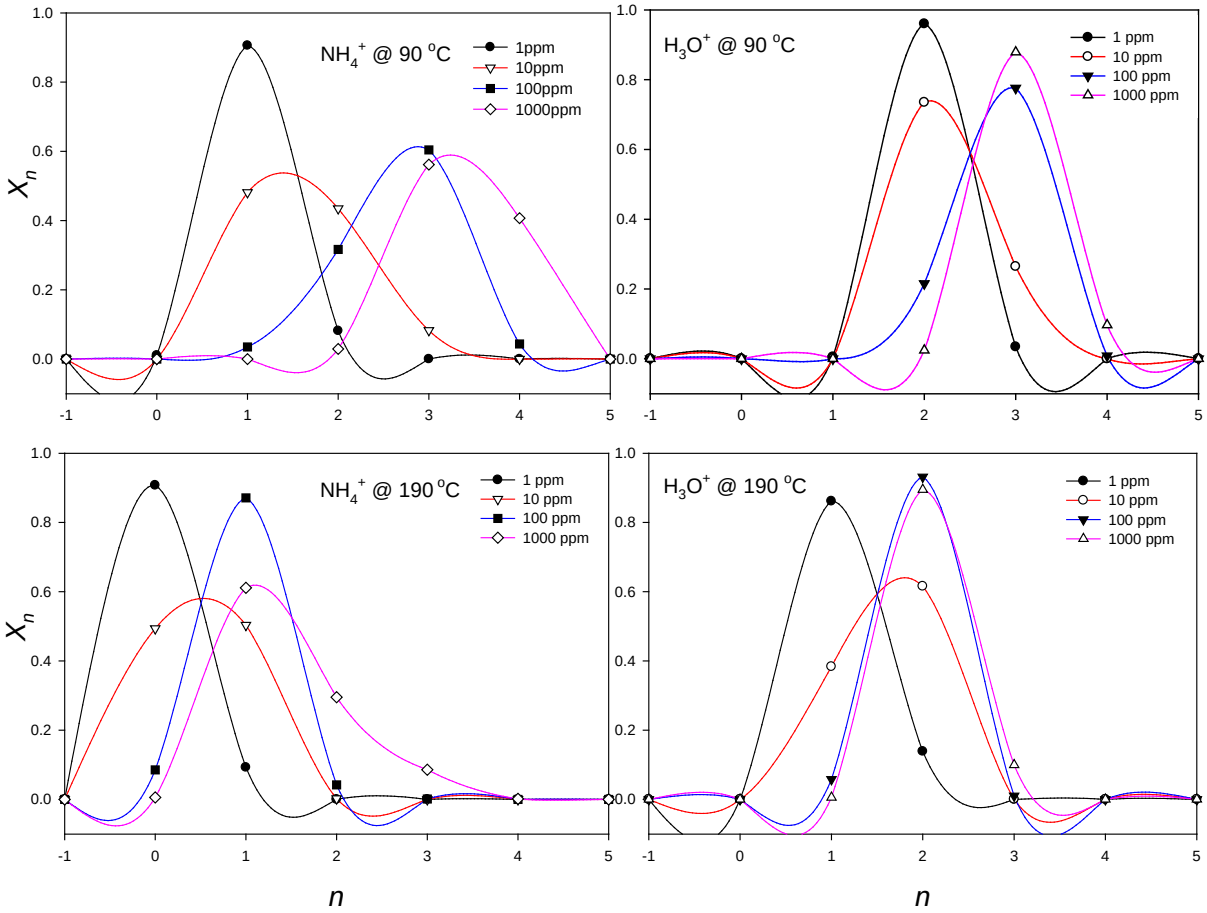

Fig.3. The relative abundances of different $NH_4^+(H_2O)_n$ and $H_3O^+(H_2O)_n$ cluster ions in the presence of 1, 10, 100 and 1000 ppm water vapor.

It is obvious that *n* is a discreet quantity and changes by one unit. The curves were plotted to demonstrate the trends of *n* in a given moisture value. Figure 3 represents the distribution of different clusters at each moisture level. The distribution moves to larger clusters as the moisture increases. This behavior is reflected in the movement of the ion mobility peak, as experimentally shown in Fig. 2. The distribution also changes with temperature. At a higher temperature of 190 °C, it generally shifts back compared to that at lower temperature of 90

°C in similar moisture level. In reality, *n* as defined by Eq. 2 starts from zero. We started *n* from a hypothetical value of -1 just for a better demonstration of the maximum distribution.

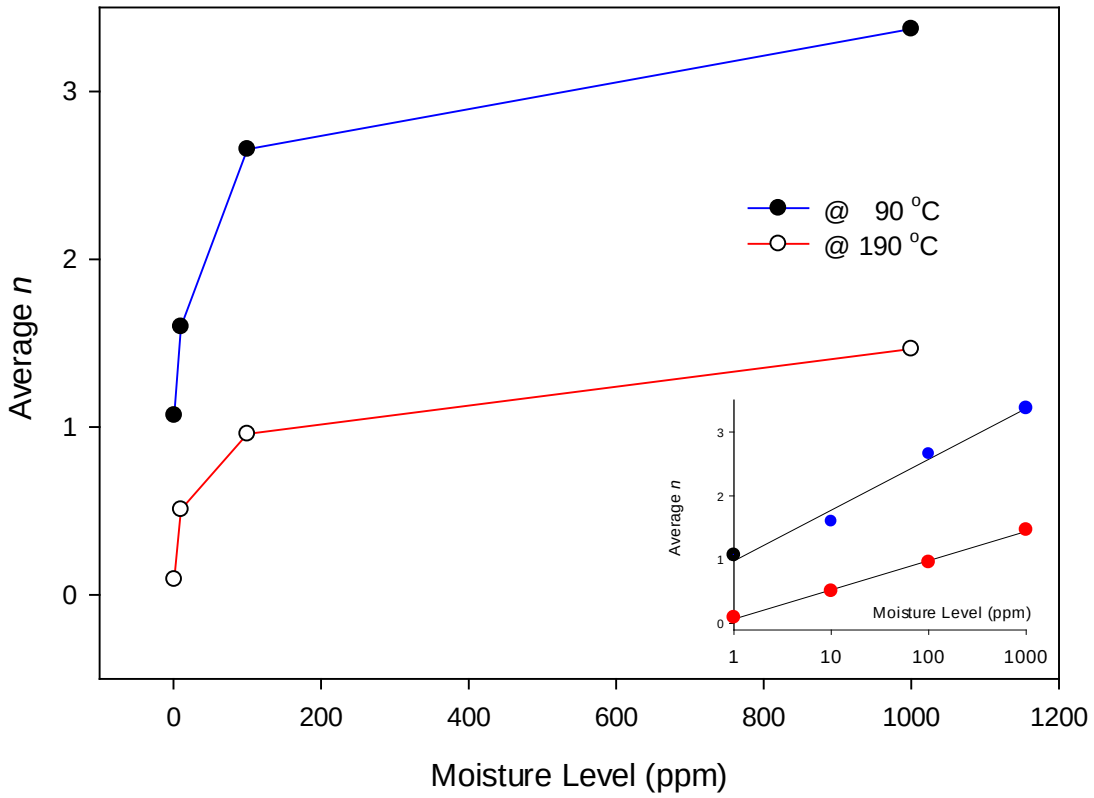

Fig.4. The average number of water clusters, *n*, for $NH_4^+(H_2O)_n$ reactant ion as a function of moisture level for two temperatures. The inset shows the average *n* versus moisture level in logarithmic scale.

The average number of water molecules at each temperature may be calculated for any moisture level using, $n_{avg}= \Sigma n.X_n$. If the results are plotted against the moisture level (see Fig. 4), it behaves very much similar to the drift times in Fig. 2b. This similarity suggests that the nature and the extent of the peak shifts in ion mobility spectra caused by moisture are directly governed by the hydration phenomenon. A similar trend was observed for other temperatures as well as for $H_3O^+(H_2O)_n$ reactant ion. Interestingly, as shown in the inset of Fig. 4, the average number of water clusters linearly changes with the logarithm of the moisture level. We will show that drift times also vary linearly with the logarithm of moisture.

4.3. Calculation of the Drift Times

Different hydrated ions with a common core ion cannot be separated in a drift tube since the adjacent hydrated species (*n* and *n*+1) rapidly interconvert to each other. In fact, all clusters travel through the drift tube continuously interconverting, ultimately coalescing into one single mobility peak. Therefore, the observed drift time is a weighted average of the drift

times of the individual ions. The average drift time for a mixture of ions traveling together depends on the individual properties of the mixture. In our recent work [29] it was proved that the average drift time, t_d is related to the single ion drift times in the form of;

$$\frac{1}{t_d} = X_0 \frac{1}{t_0^o} + X_1 \frac{1}{t_1^o} + X_2 \frac{1}{t_2^o} + \ldots . \qquad \text{(eq.5)}$$

Where X_i is the mole fraction of the i^{th} ion and t_i^o is its drift time when it travels alone. The values of mole fractions (X_i) in Eq. 5 cannot be experimentally measured by IMS, without a mass spectrometer. Hence, they are calculated from the theoretical computations using Equations 3 and 4. Yet, the drift time of each component t_i^o is unknown. It is not possible to measure individual drift times by IMS, as water vapor exists throughout the drift tube. Here, we propose a method to estimate the individual drift times.

4.3.1. The Individual Drift Times

An empirical equation in Ref. 30 relates the mass of homologous alkanes and alkenes to their mobilities as:

$$\log M = -A' K^* + b \qquad \text{(eq.6)}$$

Where A' and b are constants and K^* is the reduced mobility which is independent of the temperature. This relation is usually used to predict the approximate mass of an ion with given mobility. We use this equation to estimate the mobility or drift times for an ion with a given mass. Since our measurements were carried out at different temperatures but constant ambient pressure, the K^* is replaced with K/T in Eq. 6. Also, the mobility coefficient K is replaced by $1/t_d$; then the constant A' is changed to A.

$$\log M = -\frac{A}{T.t_d} + b \qquad \text{(eq.7)}$$

If Eq. 7 is applied for two species; including the bare core ion and its n^{th} hydrated one, we have:

$$\log \frac{M_n}{M_o} = -\frac{A}{T}\left(\frac{1}{t_n} - \frac{1}{t_o}\right) \qquad \text{(eq.8)}$$

The M_b and t_o are considered as mass and drift time of the ion with the minimum number of water molecules, i.e.the bare ion. Therefore, the drift time of each component, t_n, can be obtained as a function of the drift time of the bare ion:

$$\frac{1}{t_n} = \frac{1}{t_o} - \frac{T}{A} \log \frac{M_n}{M_o} \qquad \text{(eq.9)}$$

The mass of a hydrated ion, M_n equals to $nM_{H2O}+M_o$, thus, Eq. 9 can be rearranged to;

$$\frac{1}{t_n} = \frac{1}{t_o} - \frac{T}{A} \log(1 + nM_r) \qquad M_r = \frac{M_{H2O}}{M_o} \qquad n \geq 0 \qquad \text{(eq.10)}$$

Where M_r is the relative molecular mass of H_2O to the central ion. In the case of $H_3O^+(H_2O)_n$ ions, for example, the M_r is very close to unity and for ammonium, it is exactly one. Therefore, to a good approximation, the M_r in Eq. 10 may be removed.

4.3.2. The Overall Drift Time

If the drift times, given in Eq. 10, with eliminating M_r, are substituted in Eq. 5, the overall drift time for a mixture of hydrated ions is obtained as:

$$\frac{1}{t_d} = \sum_{n=0} X_n \left[\left(\frac{1}{t_o} - \frac{T}{A} \log(1+n) \right) \right] \qquad \text{(eq.11)}$$

Since $\sum X_n = 1$, Eq. 11 is simplified to

$$\frac{1}{t_d} = \frac{1}{t_o} - \frac{T}{A} \sum_{n=0} X_n \log(1+n) \qquad \text{(eq.12)}$$

Or:

$$\frac{1}{t_d} = \frac{1}{t_o} - \frac{T}{A} \log \prod_{n=0} (1+n)^{X_n} \qquad \text{(eq.13)}$$

Equation 13 predicts the variation of the drift time as a function of the mole fractions of the hydrated ions. In absolute dry gas, when $[H_2O]=0$, we only have the bare ion, hence, $X_0=1$ and all $X_{n>0} = 0$. Consequently, the expression $\prod_{n=0} (1+n)^{X_n}$ becomes unity and its logarithm is zero. Therefore, in absolutely dry gas, (zero moisture) the average drift time (t_d) approaches to the drift time of the bare ion. Based on Eq. 13, the drift time increases as the humidity increases.

For convenience Eq. 13 is simplified to:

$$\frac{1}{t_d} = \frac{1}{t_o} - \alpha T \log \Omega \qquad \text{(eq.14)}$$

Where α is a new constant and Ω is defined as;

$$\Omega = \prod_{n=0} (1+n)^{X_n} \qquad \text{(eq.15)}$$

The value of Ω, defined by Eq. 15, is a measure of the hydration degree of the ions. At hypothetically absolute zero moisture, the value of Ω will be unity, since n occupies only one value that is just zero and hence, all $X_{n\neq 0}$ are zero but $X_0=1$. As moisture increases, the bracket expands to higher-order clusters, and the value of Ω grows beyond unity. Mathematically, Ω never goes to infinity even at very high humidity, since the clusters distribute over many components and the mole fraction of each component becomes very small, i.e., for large n's, $X_n \rightarrow 0$. Consequently, at higher water concentrations, as the power of the bracket goes to zero, the terms corresponding to the higher order of clusters approach unity and the overall product reach a limit.

Using the data presented in Fig. 3, the values of Ω were theoretically calculated in a wide range of moisture, starting from the minimum humidity, up to 1000 ppm, at different temperatures. The results for NH_4^+ and H_3O^+ reactant ions are presented in Fig. 5. As mathematically predicted, Ω starts from one, rise rapidly, and quickly reach a plateau.

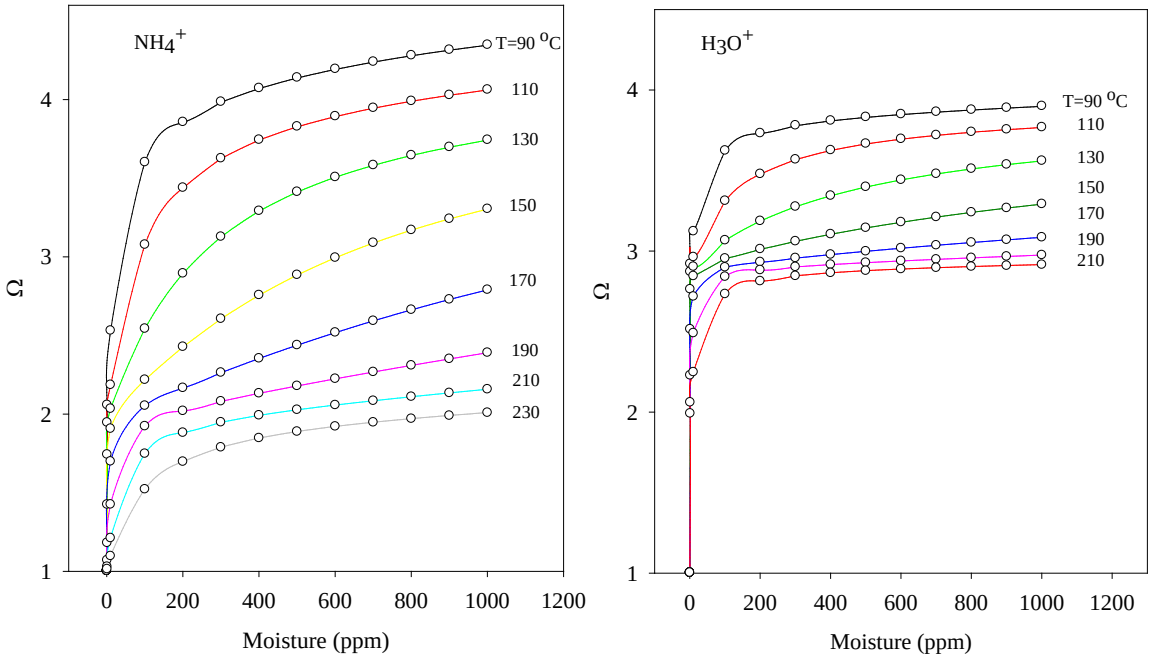

Fig. 5. Variation of Ω versus a wide range of moisture for NH_4^+ and H_3O^+ at different temperatures.

In reality, the humidity can never be zero. Specifically, from the experimental point of view and in the IMS case which operates at atmospheric pressure, water molecules diffuse into the drift region, even if a very dry gas is used. Therefore, the measured drift times never reach the absolute bare ion drift time. Here, we define a working condition in which the level of moisture in the drift tube is the lowest possible, the so-called "*dry condition*" denoted by t_{dry}. Then, the corresponding value of Ω in the dry condition would be Ω_{dry}. This may vary from instrument to instrument depending on the working conditions. Obviously, when extra moisture is added to the drift tube, the value of Ω increases. We denote the value of Ω at increased moisture level as Ω_{hum}. If Eq. 14 is applied to both dry and humid conditions, the combination yields;

$$\frac{1}{t_{hum}} = \frac{1}{t_{dry}} - \alpha T \log \frac{\Omega_{hum}}{\Omega_{dry}} \qquad \text{(eq.16)}$$

Equation 16 predicts that $1/t_d$ linearly changes with $\log(\Omega_{hum}/\Omega_{dry})$ with an intercept of $1/t_{dry}$.

4.4. Experimental Validation

Equation 16 was experimentally validated by plotting the inverse of the experimental drift times against $\Omega_{hum}/\Omega_{dry}$ in Fig. S3 presented in the supporting documents. Ω_{dry} is the calculated values of Ω at 30 ppm water concentration (the dry condition in our experiment)

and Ω_{hum} corresponds to the humidities in which the test performed. The data follow straight lines with negative slopes, confirming Eq. 16.

Obtaining the values for Ω requires complicated calculations, including, DFT, Δ*G*'s, Δ*H*'s, X_n's, and the product Π in Eq 15. We can skip those time-consuming calculations by evaluating the relationship between Ω and water concentration. Ω is a measure of the hydration of ions and it depends on the moisture. Figure 5 shows that it increases with the humidity of the drift gas. Having defined the minimum achievable humidity as the *dry condition* (30 ppm in our experiment), it is expected that the $\log(\Omega_{hum}/\Omega_{dry})$ is a function of $\log[H_2O]/[H_2O]_{dry}$ with a zero intercept. The plot of $\log(\Omega_{hum}/\Omega_{dry})$ versus $\log[H_2O]/[H_2O]_{dry}$ is shown in Fig. 6. Although the data are not perfectly linear, to a good approximation the $\log[H_2O]/[H_2O]_{dry}$ can be used instead of the $\log(\Omega/\Omega_{dry})$, especially at low water concentrations.

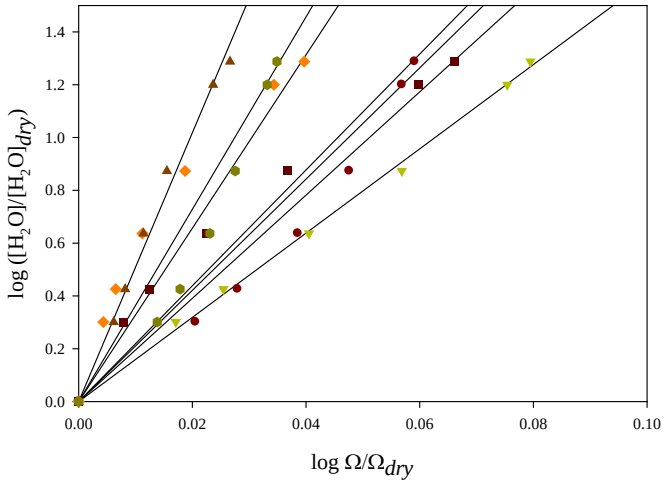

Fig. 6. The linear correlations between the $\log[H_2O]/[H_2O]_{dry}$ values and the $\log(\Omega/\Omega_{dry})$ data for NH_4^+ ion at different temperatures.

Based on the fact presented in Fig. 6, we replace $\log(\Omega_{hum}/\Omega_{dry})$ in Eq. 16 with the term $\log[H_2O]/[H_2O]_{dry}$ to give;

$$\frac{1}{t_{hum}} = \frac{1}{t_{dry}} - \beta T \log \frac{[H_2O]_{hum}}{[H_2O]_{dry}} \qquad \text{(eq.17)}$$

β is a new constant depending on temperature, the nature of the ion and the drift tube geometry. Equation 17 is a semi-empirical equation which does not need complicated and time-consuming calculations. It predicts that the reciprocal drift time changes with logarithm value of the humidity in the drift gas. The experimental results are presented in Fig. 7, where the variation of $1/t_d$ is plotted against the $\log[H_2O]/[H_2O]_{dry}$ at different temperatures for different reactant ions. The plots are all perfectly linear with negative slopes, confirming the validity of Eq. 17.

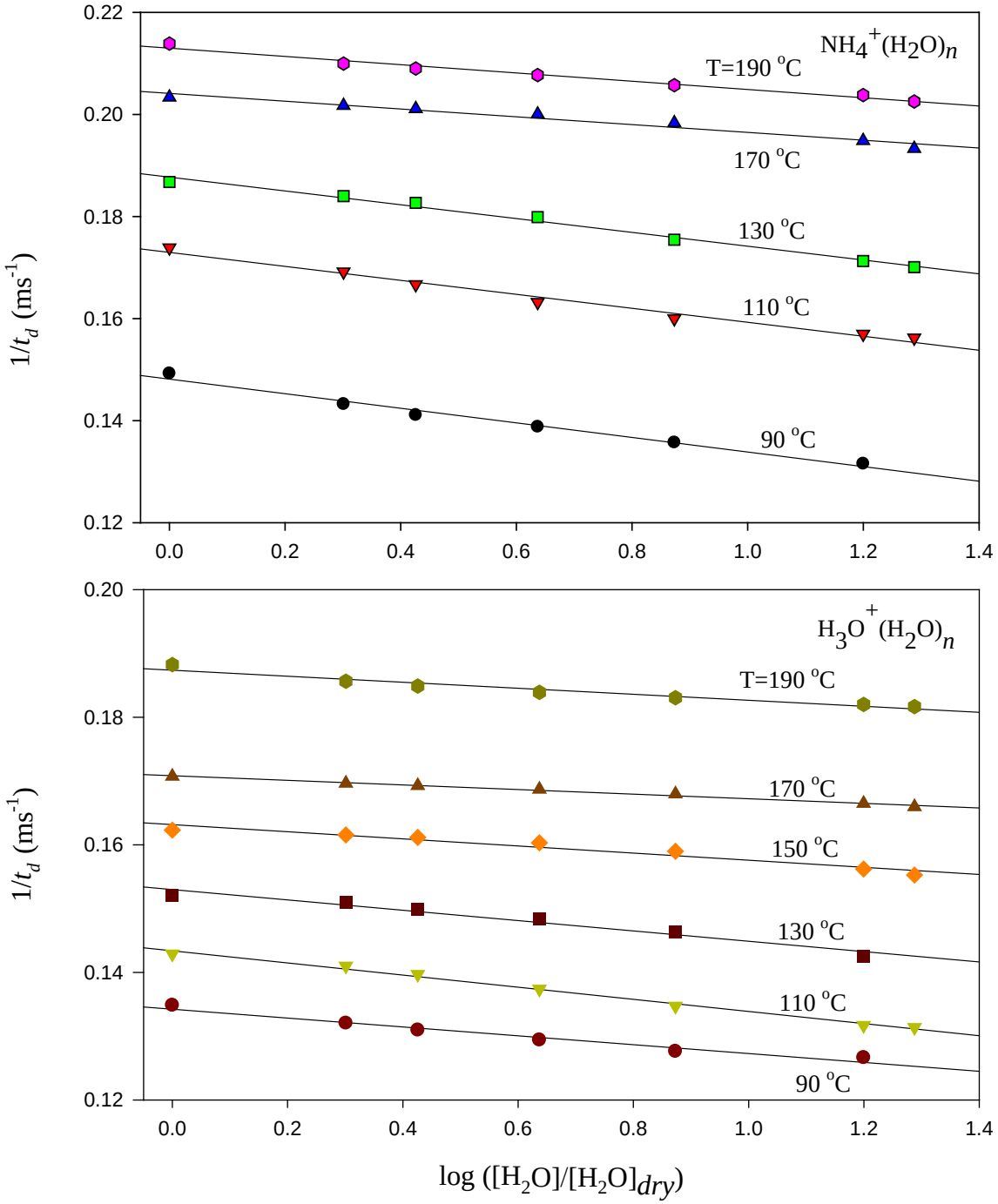

Fig. 7. The variation of $1/t_d$ as a function of $\log[H_2O]/[H_2O]_{dry}$ for NH_4^+ and H_3O^+ reactant ions at different temperatures.

The graphs are approximately parallel indicating that the slope is almost temperature-independent, but interestingly, the intercept of the graphs i.e. $1/t_{dry}$ directly depends on the temperature which is in full agreement with the reduced mobility concept.

4.5. The Standard Drift Time

We used the water concentration in the dry condition, $[H_2O]_{dry}$, as the reference for moisture, which was 30 ppm in our experiments. Since the $[H_2O]_{dry}$ is not a universal quantity, and it changes for different instruments and environments, we here define a standard condition in which the water concentration is 1 ppm. Therefore, Eq. 17 is modified to;

$$\frac{1}{t_d} = \frac{1}{t_d^{\Theta}} - \beta T \log[H_2O] \qquad \text{(eq.18)}$$

Where, t_d^{Θ} is "*the standard drift time*" when $[H_2O]$=1 ppm. The standard drift time is independent of the drift tube humidity. This value can be obtained from the extrapolation of the plot of $1/t_d$ versus the water concentration in any IMS instrument.

Eq. 18 predicts that the inverse of the reactant ions drift time changes linearly with logarithm of water concentration. This has now been proved for the positive reactant ions, $NH4^+$ and H_3O^+ that are common in both corona discharge and radioactive sources.

We also evaluated the model for the negative polarity. Since, unlike in the case of positive mode, the reactant ions in the negative corona discharge are not clear and well-separated, we used the data reported earlier [19] obtained using a Tritium source. The dependence of drift times on the humidity of the drift gas and the plot of inverse drift time versus the logarithm of water concentration is shown in Fig. 8 for the negative reactant ions and $Cl^-(H_2O)$ product ions (measurement of 1-chlorohexane at 80°C). As observed for the positive reactant ions (Fig. 2), a considerable shift of drift times can be observed for negative ions with increasing water concentrations in the drift gas (Fig. 8a). These changes in peak position vary considerably for reactant ions and chlorinated product ions due to different tendencies to form water clusters. Fig. 8b clearly shows that the data for the negative reactant ions and product ions also confirm the model. Reciprocal drift time changes correlate linearly with logarithm value of the humidity in the drift gas. Therefore, these data from negative measurements perfectly fit into the model developed here.

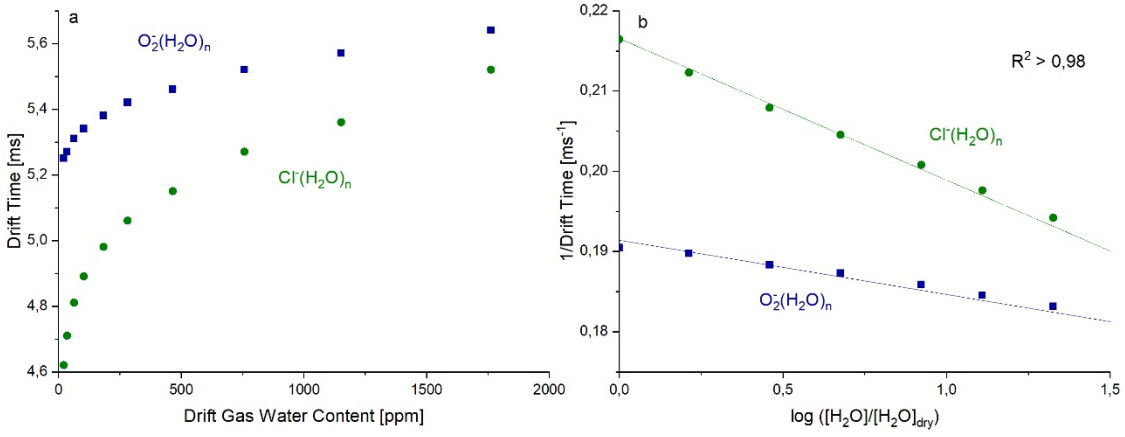

Fig. 8. The effect of water concentration on the drift time (a) and variation of $1/t_d$ as a function of $\log[H_2O]/[H_2O]_{dry}$ (b) for $O_2^-(H_2O)_n$ reactant ions and $C^-(H_2O)_n$ product ions

4.6. The Standard mobility

As $1/t_d$ gives the mobility, standard mobility, K^{Θ} can be defined here, similar to the standard drift time definition. This standard mobility is independent of the moisture level of the drift gas, just as K_0, the reduced mobility, that is independent of the temperature and pressure. Hence,

$$K= K^{\Theta} - \gamma T \ ln[H_2O] \quad \text{(eq. 19)}$$

The ionic mobility in this equation may be compared with the chemical potential, μ, that has a similar formula and a comparable behavior with pressure, P, as;

$$\mu=\mu^{\Theta}+ RT \ ln \ P \quad \text{(eq. 20)}$$

The standard chemical potential is defined when the pressure is 1 bar. The standard mobility is also defined when the water concentration is 1 ppm. On the other hand, the chemical potential decreases when the pressure drops. Since P relates to $1/V$ at constant temperature, $ln \ P \propto -ln \ V$ and eq. 20 can be shown in terms of volume as $\mu \propto \mu^{\Theta} - RT \ ln \ V$. This means that expanding the volume results in decreasing the chemical potential. Similarly, the mobility decreases when the amount of $[H_2O]$ increases. It seems that the water concentration here plays a role, similar to the volume in the gas-phase case. Increasing the volume provides more space for the gaseous molecules to dilute themselves. In a similar manner, increasing the moisture gives more room to the ions to expand themselves in different forms of hydration. In fact, both the volume and the water concentration increase the entropy of the system. This, not only reduces the average mobility of the ion but also decreases its chemical reactivity. The hydrated reactant ions do not tend to react with the sample molecules, as the charge is distributed over a large number of water molecules around the core ion. Therefore, the sensitivity of IMS is reduced at elevated moisture levels. Actually, K or mobility of a specific reactant ion may be regarded as its chemical reactivity in comparison with its dry form of K^{Θ} having the highest reactivity.

4.7. The Entropy

The Boltlzmann's entropy formula, given in Eq. 21, shows the relationship between entropy, S, and ω, the number of ways of a thermodynamic system can be arranged.

$$S = k \ln \omega \quad \text{(eq. 21)}$$

The lowest value of ω is one. Hence, the minimum entropy or maximum order happens for a system when there is only one way of arranging. This usually happens at absolute zero temperature for an ideal crystal. The parameter Ω, defined in eq.15 has the same meaning as ω in Eq. 21. It reflects the number of ways that the reactant ion can exist in the form of clusters. At hypothetically zero moisture, Ω=1 and there exists only one way for the reactant ions to appear, which is just the bare ion. This creates the highest order in the system. At elevated moistures, other possible forms or higher-order clusters are available to be populated. The entropy here is reflected in the drift time. The more entropy of the system, the longer drift time of the reactant ion. As a matter of fact, the presence of water opens other channels for the ion to exist as different hydration forms. This broadens the distribution and cause disorder. Similar to the Boltzmann's relation, Eq. 14 demonstrate a logarithmic

connection between entropy and probability. This concept is the subject of an independent study in the field of ion clusters.

5. Conclusion

There can be no doubt that, in IMS, the peaks shift to the higher drift times as the humidity of the drift gas increases. This is due to the hydration of ions at atmospheric pressure. The displacement of the reactant ion peak positions was formulated as a function of the relative abundances, of the hydrated ions which depend on the humidity. To avoid theoretical computations of the relative abundances the model was modified to give the drift time as a function of the moisture or water concentration.

The measured mobilities are corrected to a standard temperature and pressure and are usually reported as the reduced mobility. However, there are considerable discrepancies among the reported values. Part of this inconsistency is due to the different humidity levels of the instruments used for measurement. Therefore, standard mobility, K^{Θ} ,which is independent of the moisture level of the drift gas, was defined. This definition may be extended to "*the standard reduced mobility*" K_o^{Θ} value.

Although, we mainly focused on the reactant ions in this work, the argument may be extended to the product ions. However, the product ions are, to a lesser extent, hydrated. The preliminary results show that the drift time of the product ions also changes logarithmic with the moisture level which is the subject of our the next study. The model can also be extended to the modifiers added to the drift gas that enhances the separation. As the separation between the peaks also differs at different moisture levels, this can be used as an indication of the moisture level in the drift tube.

The effect of humidity was finally viewed in the context of the entropy concept. It was attributed to the distribution of ions in the possible hydration forms. Accurate experimental evaluation to this theory can be achieved by population study of ion clusters with a mass spectrometer at different moisture levels.

Acknowledgments

Financial support was provided by the Isfahan University of Technology. Authors would like to thank the Dalian Institute of Chemical Physics and the Chinese Academy of Sciences for their hospitality and providing facilities and conveniences through the CAS President's International Fellowship Initiative (Grant No. 2019VEA0033). Furthermore, we cordially thank, Malcolm Cämmerer, for proofreading the manuscript.

References

[1]Eiceman, G.A.; Karpas, Z., *Ion Mobility Spectrometry*, 2nd edition, CRC Press, Boca Raton, FL, 2005.

[2] Borsdorf, H.; Eiceman, G.A., Ion mobility spectrometry: principles and applications, *Appl. Spectrosc. Rev.* 2006, 41, 323–375.

[3] M. Tabrizchi, V. Ilbeigi, Detection of explosives by positive corona discharge ion mobility spectrometry J. Hazard. Mater. 2010, 176, 692-696.

[4] Ewing, R.G.; Atkinson, D.A.; Eiceman, G.A.; Ewing, G.J., A critical review of ion mobility spectrometry for the detection of explosives and explosive related compounds, *Talanta*, 2001, 54, 515–529.

[5] Pozzi, R.; Bocchini, P.; Pinelli, F.; Galletti, G.C., Rapid analysis of tile industry gaseous emissions by ion mobility spectrometry and comparison with solid phase micro-extraction/gas chromatography/mass spectrometry, *J. Environ. Monit*. 2006, 8(12), 1219–1226.

[6] Marquez-Sillero, I.; Aguilera-Herrador, E.; Cardenas, S.; Valcarcel, M., Ion-mobility spectrometry for environmental analysis, *Trends Anal. Chem.* 2011, 30, 677–690.

[7] Makinen, M.A.; Anttalainen, O.A.; Sillanpaa, M.E.T., Ion mobility spectrometry and its applications in detection of chemical warfare agents, *Anal. Chem.* 2010, 82, 9594–9600.

[8] Steiner, W.E.; Klopsch, S.J.; English, W.A.; Clowers, B.H.; Hill, H.H., Detection of a chemical warfare agent simulant in various aerosol matrixes by ion mobility time-of-flight mass spectrometry, *Anal. Chem.* 2005, 77, 4792–4799.

[9] Eiceman, G.A.; Krylov, E.V.; Tadjikov, B.; Ewing, R.G.; Nazarov, E.G.; Miller, R.A., Differential mobility spectrometry of chlorocarbons with a micro-fabricated drift tube, *Analyst* 2004, 129, 297–304

[10] H. Borsdorf, T. Mayer, Temperature dependence of ion mobility signals of halo-genated compounds, Talanta 101 (2012) 17–23.

[11] M. Tabrizchi, Temperature Corrections for Ion Mobility Spectrometry, Applied Spectroscopy, 55(2001)1653-1659.

[12] M. Tabrizchi, Temperature effects on resolution in ion mobility spectrometry, Talanta 62 (2004) 65–70.

[13] M. Tabrizchi, F. Rouholahnejad, Pressure effects on resolution in ion mobility spectrometry, Talanta 69 (2006) 87–90.

[14] E.J. Davis, P. Dwivedi, M. Tam, W.F. Siems, H.H. Hill, High-pressure ion mobility spectrometry, Anal. Chem. 81 (2009) 3270–3275.

[15] V. Bocos-Bintintan, A. Brittain, C. L. P. Thomas, The response of a membrane inlet ion mobility spectrometer to chlorine and the effect of water contamination of the drying media on ion mobility spectrometric responses to chlorine, Analyst126 (2001) 1539–1544.

[16] M. Mäkinen, M. Sillanpää, A.-K. Viitanen, A. Knap, J.M. Mäkelä, J. Puton, “The effect of humidity on sensitivity of amine detection in ion mobility spectrometry”, Talanta 84 (2011) 116–121.

[17] W. Vautz, V. Ruszany, S. Sielemann, J. Baumbach, Sensitive ion mobility spectrometry of humid ambient air using 10.6 eV UV-IMS, Int. J. Ion Mobil. Spectrom.7 (2004) 3–8.

[18] W. Vautz, S. Sielemann, J. I. Baumbach, Determination of terpenes in humid ambient air using ultraviolet ion mobility spectrometry, Anal. Chim. Acta 513(2004) 393–399.

[19] T. Mayer, H. Borsdorf, Accuracy of Ion Mobility Measurements Dependent on the Influence of Humidity, Anal. Chem. 2014, 86, 5069−5076.

[20] H. Borsdorf, P. Fiedler, T. Mayer, The effect of humidity on gas sensing with ion mobility spectrometry, Sensors and Actuators B: Chemical, 218 (2015) 184–190

[21] BO. Zhang, Jinliang He, Dependence of the Average Mobility of Ions in Air with Pressure and Humidity, IEEE Transactions on Dielectrics and Electrical Insulation, 24(2017) 923-928.

[22] Z. Safaei, G. A. Eiceman, J. Puton, J.A. Stone, M. Nasirikheirabadi, O. Anttalainen, M. Sillanpää, Scientific Reports 9(2019) 5593.

[23] Z. Izadi, M. Tabrizchi, H. Farrokhpour, Thermodynamic study of proton-bound dimers formation in atmospheric pressure: An experimental and theoretical study, J. Chem. Thermodynamics 63 (2013) 17-23.

[24] Y. Valadbeigi, H. Farrokhpour, M. Tabrizchi, Effect of Hydration on the Kinetics of Proton-bound Dimer Formation: An Experimental and Theoretical Study, J. Phys. Chem. A, 2014, 118, 7663-7671.

[25] M. J. Frisch, G. W. Trucks, H. B. Schlegel, G. E. Scuseria, M. A. Robb, J. R. Cheeseman, G. Scalmani, V. Barone, B. Mennucci, G. A. Petersson, H. Nakatsuji, M. Caricato, X. Li, H. P. Hratchian, A. F. Izmaylov, J. Bloino, G. Zheng, J. L. Sonnenberg, M. Hada, M. Ehara, K. Toyota, R. Fukuda, J. Hasegawa, M. Ishida, T. Nakajima, Y. Honda, O. Kitao, H. Nakai, T. Vreven, J. A. Montgomery, Jr., J. E. Peralta, F. Ogliaro, M. Bearpark, J. J. Heyd, E. Brothers, K. N. Kudin, V. N. Staroverov, R. Kobayashi, J. Normand, K. Raghavachari, A. Rendell, J. C. Burant, S. S. Iyengar, J. Tomasi, M. Cossi, N. Rega, J. M. Millam, M. Klene, J. E. Knox, J. B. Cross, V. Bakken, C. Adamo, J. Jaramillo, R. Gomperts, R. E. Stratmann, O. Yazyev, A. J. Austin, R. Cammi, C. Pomelli, J. W. Ochterski, R. L. Martin, K. Morokuma, V. G. Zakrzewski, G. A. Voth, P. Salvador, J. J. Dannenberg, S. Dapprich, A. D. Daniels, O. Farkas, J. B. Foresman, J. V. Ortiz, J. Cioslowski, and D. J. Fox, Gaussian 09, Revision A.1., Gaussian, Inc.: Wallingford, 2009.

[26] M. Tabrizchi, T. Khaymian, N. Taj, Design and optimization of a corona discharge ionization source for ion mobility spectrometry, Rev. Sci. Instrum. 71 (2000) 2321-2328.

[27] M. Tabrizchi, T. Khaymian, N. Taj, Design and optimization of a corona discharge ionization source for ion mobility spectrometry, Rev. Sci. Instrum. 71 (2000) 2321-2328.

[28] P.W. Atkins, Physical Chemistry, Oxford University Press, Oxford, 2017.

[29] Z. Izadi, M. Tabrizchi, H. Farrokhpour, Average drift time and average mobility in ion mobility spectrometry, Int. J. Mass Spectrometry, 412 (2016) 20-25.

[30] H. Borsdorf, H. Schelhorn, J. Flachowsky, H. R. Doring, J. Stach, Corona discharge ion mobility spectrometry of aliphatic and aromatic hydrocarbons, Anal. Chim. Acta 403 (2000) 235-242.